Absorption Spectra and Electron Injection Study of the Donor Bridge Acceptor Sensitizers by Long Range Corrected Functional

Irfan, Ahmad*+

Department of Chemistry, Faculty of Science, King Khalid University, Abha 61413, P.O. Box 9004, SAUDI ARABIA

ABSTRACT: *Ground state geometries have been computed using Density Functional Theory (DFT) at B3LYP/6-31G(d,p) level of theory. The excitation energies and spectroscopic parameters have been computed using Long range Corrected (LC) hybrid functional by Time Dependent Density Functional Theory (TDDFT) with LC-BLYP level of theory. The Polarizable Continuum Model (PCM) has been used for evaluating bulk solvent effects at all stages. The efficient materials have been predicted and electron injection (ΔG^{inject}), electron coupling constant ($|V_{RP}|$) and Light Harvesting Efficiency (LHE) has been discussed. By elongating the bridge all these three parameters ΔG^{inject}, $|V_{RP}|$ and LHE enhanced which revealed that new designed sensitizers would be efficient.*

KEY WORDS: *Dye-sensitized solar cells, Absorption, Light harvesting efficiency, Electronic coupling constant, Electron injection.*

Archive of SID

INTRODUCTION

Dye Sensitized Solar Cells (DSCs) are currently attracting considerable attention because of their high light-to-electricity conversion efficiencies, ease of fabrication, and low production costs [1]. Following their inception in 1985 [2], DSCs are often included in the Organic PhotoVoltaic (OPV) family because of the organic nature of at least part of its constituents. The DSC is the only photovoltaic device that uses molecules to absorb photons and convert them to electric charges without the need of intermolecular transport of electronic excitation. It is also the only solar cell that separates the two functions of light harvesting and charge-carrier transport, whereas conventional and all of the other known OPV devices perform both operations simultaneously. In the DSC, the recombination of charge carriers occurs across the phase boundary separating the electron from the hole conductor medium. This inherent geometry offers the unique prospective to fashion the interface in a judicious manner to retard the back-electron-transfer reaction. One promising approach to accomplish this goal is the molecular engineering of sensitizers forming a self-assembled compact monolayer alone or in conjunction with a co-adsorbent at the oxide surface. Such an insulating film would impair the flow of dark current across the junction, reducing the back-reaction rate and increasing the overall solar to electric power conversion efficiency of the cell.

However, most of these devices generally consist of expensive sensitizers such as ruthenium (II) polypyridyl

* To whom correspondence should be addressed.
+ E-mail: irfaahmad@gmail.com
Other Address: Center of Excellence for Advanced Materials Research, King Khalid University, P.O. Box 9004, Abha 61413, SAUDI ARABIA
1021-9986/14/2/11 18/$/3.80

www.SID.ir

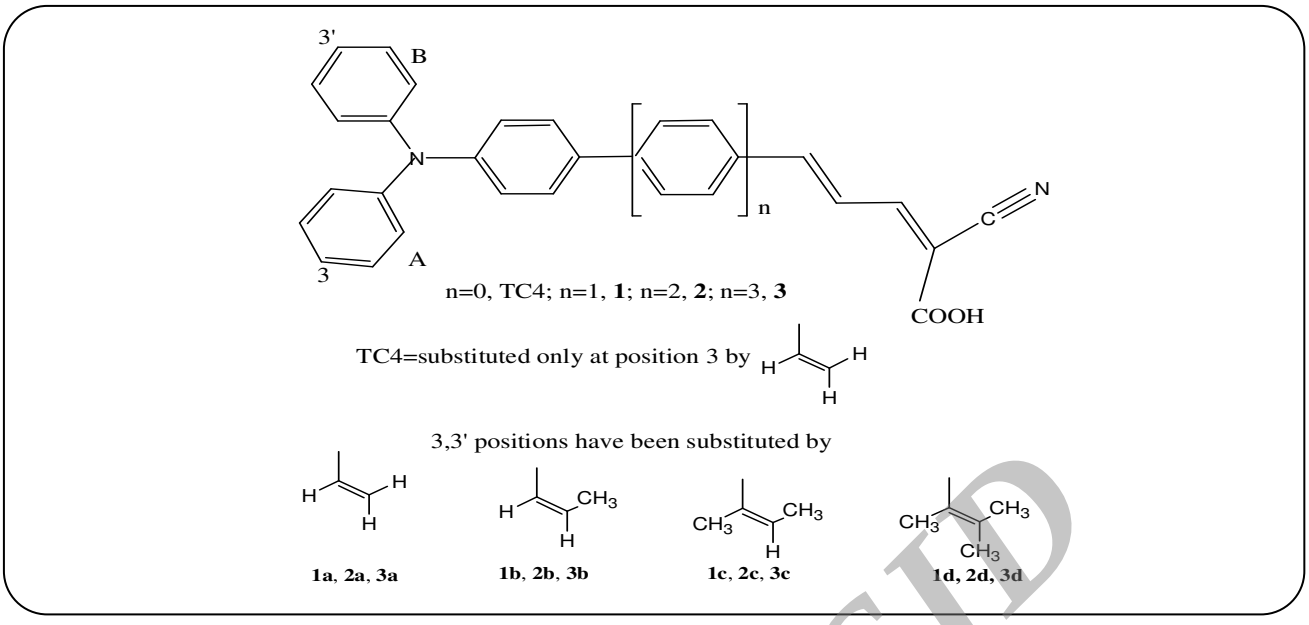

Fig. 1: The structures of 1a-3d investigated in the present study.

complexes (with carboxylated ligands) and electrolytes with volatile solvents [1,3]. Most of the organic sensitizers applied in DSCs have three important parts: 1) the electron donor such as the indoline moiety, 2) the electron acceptor such as the rhodanine ring, and 3) the linker units for the pi conjugation to enhance the molar absorption coefficient [4]. Generally, organic dyes for excellent DSCs are required to possess broad and intense spectral absorption in the visible light region and have suitable excited-state redox potential with the energy of the conduction band edge. The major factors in the low conversion efficiency of DSCs based on organic dyes are the formation of dye aggregation on the semiconductor surface and the recombination of conduction band electrons with triiodide in the electrolyte [5]. The Ru complexes photosensitizers show a solar energy to electricity conversion efficiency of 10% in average. Nevertheless, an increasing interest for purely organic DSCs as substitutes for Ru complexes raised in recent years due to their key advantages, e.g. a high molar extinction coefficient, a simple and relatively inexpensive preparation processes, a more straightforward compliance with environmental rules [6]. Moreover, several solid-state DSCs based on organic dyes appear to have equivalent performances than inorganic complexes, suggesting promising commercial applications [7]. Therefore, metal-free dyes like coumarin [8], merocyanine [9], indoline [10], xanthenes [11], hemi-cyanine [12], hydroquinones [13,14] perylene [15], fluorine [16] and triphenylamine (TPA) [17] have been tested in this framework.

To model and design efficient metal-free sensitizers for DSCs, appropriate Donor Bridge Acceptor (DBA) systems are required whose properties can be tuned by applying the passable structural modifications. The DSC based on 2-cyano-5-(4-(phenyl(4-vinylphenyl) amino)phenyl) penta-2,4-dienoic acid (TC4) showed efficiency 4.82% [17a]. Xu et al. attached vinyl unit at position 3 of A-ligand to enhance the electron-donor ability of TPA [17a]. In the present study we designed DBA systems where TPA moiety as donor, cyanoactetic acid as acceptor and benzene rings (extended 1-3 in number) as bridge. In our previous study it was examined that positions 3 (A-ligand) and 3` (B-ligand) are favorable to design better sensitizer [17b]. Thus in the present study not only we have substituted the vinyl at position 3 and 3`, we have also modeled new systems by replacing the hydrogens of vinyl with CH_3 to enhance the donor ability of TPA moiety, see Fig. 1 (detail can be found in computational details). The Quantum chemical calculations have been performed to gain insight into electronic properties of the new designed sensitizers. The structure-property relationship has been discussed.

Archive of SID

www.SID.ir

Computational detail

The ground state geometries have been computed using Density Functional Theory (DFT) with Gaussian09 package [18]. The orbital energies have been accurately predicted by reparametrization of the Becke-3 hybrid exchange-correlation functional [19,20] *Preat et al.* optimized the ground state geometries of the TPA based dyes at B3LYP/6-31G(d,p) level of theory. They concluded that this level of theory is adequate for TPA based sensitizers [21,22]. *Xu et al.* optimized TC4 by means of the B3LYP/6-31G(d,p) level of theory. The B3LYP/6-31G(d,p) level has been used for geometrical and electronic properties of the TC4 [17a]. The geometries of TPA based sensitizers have been optimized by using different Pople basis sets as 6-31G(d,p), 6-31+G(d,p), 6-311G(d,p), 6-31G(2d,2p), 6-311G(2d,2p), and 6-311G(2df,2pd) [22]. It was concluded that the B3LYP bond lengths do not depend upon the basis set and are almost identical to the MP2/6-31G(d,p) values [22]. They validated B3LYP for optimizing the geometry of TPA based sensitizers. Moreover, B3LYP/6-31G(d,p) level which is adequate for TPA based sensitizers has been applied to optimize the ground state geometries and shed light on the electronic properties [21-26]. Thus in the present study, ground state geometries have been computed by using popular three parameter B3LYP functional [23], in which the exchange is a combination of Hartree-Fock exchange, Slater functional, and Becke's Generalized Gradient Approximation (GGA) correction [24], whereas the correlation part combines local and Lee Yang Parr (LYP) functional [25]. We have used 6-31G(d,p) [17b, 26] basis set for the ground-state geometries.

Stein et al. studied the charge-transfer excitations in a series of coumarin-based donor-bridge-acceptor dyes. They explained that excitation energies well reproduced by using a range-separated hybrid functional within the generalized Kohn Sham approach to TDDFT [27]. The absorption and fluorescence properties in a class of oligothiophene push pull biomarkers have been investigated with a Long range Corrected (LC) density functional method [28]. The excited-state properties in a series of coumarin solar cell dyes were investigated with LC-BLYP [29]. The range-separation technique is based on a more physical model of the exchange potential. The B3LYP hybrid functional underestimates vertical excitation energies, especially for larger dye molecules. As a benchmark study, we have computed the absorption spectra of TC4 at TD-B3LYP/6-31G** level of theory in methanol, the absorption spectra was overestimated, i.e., 526 nm compared to experimental data 425 nm. It has been already reported that the choice of the range separation parameter is strongly system dependent [30-33], The long range (LC-BLYP) has been applied to investigate the excitation energies for TPA based dyes. In our investigated systems organic sensitizers consisted electron donor and acceptor separated from each other by conjugated units. Thus we have used LC-BLYP range separated functional. The electronic absorption spectra require calculation of the allowed excitations and oscillator strengths. The TDDFT was used to investigate the absorption properties of molecules which have been proved an efficient approach [34-36]. The iodine/iodide couple is used as regenerator in DSCs, implying that the solar cells work in solvent phase. Thus UV/Vis experimental data for TPA-based dyes are reported in solvent. The polarizable continuum model (PCM) [37-40] is used for evaluating bulk solvent effects at all stages. The calculations have been carried out in methanol according to the experimental set up [17a].

Molecular orbitals were visualized by using Gaussview. To enhance the electron donor ability of TPA moiety Xu et al. synthesized the TC4 where vinyl unit has been substituted at position **3** [17]. Recently, we showed that substitution of vinyl at position **3** and **3'** are more favorable toward enhancing the electron injection and reducing the HOMO-LUMO energy gap [17b]. It is well known that CH_3 enhance the electron donor ability [34] and the sensitizers where charge transferred from donor to acceptor moiety are good towards high efficiency [22,23]. Thus to augment the donor ability of TPA unit, we have replaced the hydrogens of vinyl by CH_3. We substituted positions 3,3' by vinyl (**1a**, **2a** and **3a**), in second step, we have replaced one hydrogen by CH_3 (**1b**, **2b** and **3b**), third step we substituted two CH_3 (**1c**, **2c** and **3c**) and finally three CH_3 were substituted in place of three hydrogens (**1d**, **2d** and **3d**) of vinyl at positions **3** and **3'**. Moreover, to check the effect of bridge on the electronic properties we have extended the benzene rings; one benzene ring between TPA moiety and anchoring group (**1**), two benzenes (**2**) and three benzenes as bridge (**3**).

Archive of SID

www.SID.ir

*Table 1: The absorption wavelength (λ_a), ΔG^{inject}, oxidation potential, Light Harvesting Efficiency (LHE), $|V_{RP}|$ of investigated dyes at TD-LC-BLYP//B3LYP/6-31G** and PCM- B3LYP/6-31G** level of theory.*

System	λ_a	ΔG^{inject}	ΔG_r^{inject}	E_{OX}^{dye} E_{OX}^{dye}	$E_{OX}^{dye^*}$	λ_{max}^{ICT}	f	LHE	$\|V_{RP}\|$
1a	348	-2.53	1.20	5.03	1.47	3.56	2.1805	0.9934	1.265
1b	349	-2.63	1.25	4.92	1.37	3.55	2.1873	0.9935	1.315
1c	349	-2.60	1.23	4.95	1.40	3.55	2.1371	0.9927	1.300
1d	349	-2.58	1.22	4.97	1.42	3.55	2.1271	0.9925	1.290
2a	341	-2.71	1.28	4.93	1.29	3.64	2.3668	0.9957	1.355
2b	341	-2.78	1.32	4.86	1.22	3.64	2.3557	0.9956	1.390
2c	341	-2.73	1.29	4.91	1.27	3.64	2.3269	0.9953	1.365
2d	341	-2.75	1.30	4.88	1.25	3.63	2.3302	0.9953	1.375
3a	339	-2.76	1.31	4.90	1.24	3.66	2.4158	0.9962	1.380
3b	339	-2.83	1.34	4.82	1.17	3.65	2.4146	0.9961	1.415
3c	339	-2.79	1.32	4.86	1.21	3.65	2.3956	0.9960	1.395
3d	339	-2.82	1.34	4.83	1.18	3.65	2.3996	0.9960	1.410
TC4	373	-2.11	1.00	5.22	1.89	3.33	1.7622	0.9827	1.055

RESULTS AND DISCUSSION

Absorption

The absorption spectra of TC4 has been computed at PCM-TD-LC-BLYP/6-31G** and PCM-TD-B3LYP/6-31G** level of theories. The PCM-TD-B3LYP overestimates the absorption wavelength about 101 nm compared to experimental maximum absorption wavelength. The maximum absorption wavelength at PCM-TD-LC-BLYP/6-31G** is 373nm which better reproduce the experimental evidence. Thus we have computed the absorption spectra of new designed sensitizers at PCM-TD-LC-BLYP/6-31G** level of theory. In addition, the absorption wavelengths of **1a**-**1d** are 25 nm blue shifted, see Table 1. The maximum absorption wavelength of **2a**-**2d** is 32 nm while **3a**-**3d** is 34 nm blue shifted compared to TC4. The excitation energies, absorption wavelengths, oscillator strengths and transition contribution are listed in Table 1 and Fig. S1 (see supporting information). Electronic transitions up to 10 states were studied for all new designed sensitizers.

In **TC4**, the maximum transition for first state is caused by HOMO ->LUMO with 70% contribution. The second state caused by HOMO ->LUMO+1 with 62% contribution. The seventh state has 55% contribution from HOMO-8 ->LUMO. The transition contribution for third, fourth, fifth, sixth, eighth, ninth and tenth states for all the frontier molecular orbitals is less than 50%.

In **1a**, S0-S1 state remains dominated with maximum absorption and this state is caused by HOMO-1 ->LUMO with 55% contribution. The second state caused by HOMO ->LUMO+1 with 77% contribution. The fifth state showed 51% contribution from HOMO-6 ->LUMO. The third, fourth, sixth, seventh, eighth, ninth and tenth states have less than 50% contribution for transitions. In **1b** the main transitions having more than 50% contributions are as follows: HOMO-1 ->LUMO for first state (53%), HOMO ->LUMO+2 for third state (70%), HOMO->LUMO+3 for fourth state (60%). In **1c**, S0-S1 transition is caused by HOMO-1 ->LUMO with 51% contribution. Maximum absorption has been observed in this state. Transition of third state is dominated with 75% contribution from HOMO -> LUMO+2. Transitions in fourth and ninth states are mainly caused by HOMO ->LUMO+3, and HOMO-11->LUMO, with the contribution of 66% and 54%, respectively. Other states of this molecule have major contribution less than 50%. In **1d**, S0-S1 state remains dominated with maximum absorption and this state is caused by HOMO-1 ->LUMO with 50% contribution. The third state caused by HOMO ->LUMO+2 with 69% contribution. The fourth

Archive of SID

www.SID.ir

state has 64% contribution from HOMO->LUMO+3. The ninth state caused by HOMO-11 ->LUMO with 55% contribution. The second, fifth, sixth, seventh, eighth, and tenth states are derived from frontier orbitals having contribution less than 50%.

In **2a**, S0-S1 state remains dominated with maximum absorption spectrum which is caused by HOMO-1 ->LUMO with 66% contribution. The second state caused by HOMO ->LUMO+1 with 52% contribution. The third state has 76% contribution from HOMO->LUMO+2. The fourth state has 57% contribution from HOMO->LUMO+4. The fifth, sixth, seventh, eighth, ninth and tenth states have less than 50% contribution from which these have been derived. In **2b**, S0-S1 state remains dominated with maximum absorption and this state is caused by HOMO-1 ->LUMO with 65% contribution. The third state caused by HOMO ->LUMO+2 with 78% contribution. The fourth state has 66% contribution from HOMO->LUMO+4. The fifth state caused by HOMO-9 ->LUMO with 54% contribution. In **2c**, S0-S1 state remains dominated with maximum absorption and this state is caused by HOMO-1 ->LUMO with 65% contribution. The third state has 78% contribution from HOMO->LUMO+2. The fourth state caused by HOMO ->LUMO+3 with 67% contribution. The fifth state caused by HOMO-9->LUMO with 54% contribution. The tenth state has 54% contribution from HOMO-13 ->LUMO. In **2d**, S0-S1 state remains dominated with maximum absorption and this state is caused by HOMO-1 ->LUMO with 64% contribution. The third state has 74% contribution from HOMO->LUMO+2. The fourth state caused by HOMO ->LUMO+3 with 67% contribution. The fifth state caused by HOMO-10 ->LUMO with 54% contribution. The tenth state has 54% contribution from HOMO-13 ->LUMO.

The main transition in **3a** is HOMO-1 ->LUMO with the contribution 57%. The HOMO ->LUMO+2, HOMO ->LUMO+4, and HOMO-9 ->LUMO transition are responsible for 3rd, 4th and 6th state with the contribution 77%, 56% and 55%, respectively**.** In **3b** main transition showed contribution 56% is responsible for HOMO-12 ->LUMO. The major contributors of this system in each state having contribution more than 50% are as follows, HOMO->LUMO+2, HOMO ->LUMO+4, HOMO-10 ->LUMO, having contribution 77%, 68% and 55% for 3rd, 4th, and 6th states. In **3c**, S0-S1 state remains dominated with maximum absorption and this state is caused by HOMO-1 ->LUMO with 58% contribution. The third state has 76% contribution from HOMO->LUMO+3. The fourth state caused by HOMO ->LUMO+4 with 69% contribution. The sixth state has 55% contribution from HOMO-11 ->LUMO. In **3d**, S0-S1 state remains dominated with maximum absorption and this state is caused by HOMO-1 ->LUMO with 57% contribution. The third state caused by HOMO->LUMO+3 with 75% contribution. The 55% contribution has been observed for sixth state transition from HOMO-12 ->LUMO.

It is noteworthy that in all these new designed molecules S0-S1 state show maximum absorption and this state is mainly derived from HOMO-1 -> LUMO transition. In fact, the maximum absorption wavelength (λmax abs) is red shifted and the oscillator strength increases from 1.7622 to reach 2.4158 in new modeled sensitizers compared to TC4.

Electron injection

The description of the electron transfer from a dye to a semiconductor, the rate of the charge transfer process can be derived from the general classical Marcus theory, [34,41-43].

$$k_{inject} = |V_{RP}|\ (2/h\ (\pi/\lambda k_B T)1/2 \exp[-(\Delta G^{inject} + \lambda)2/4\lambda k_B T] \quad (1)$$

In eq. (1), k_{inject} is the rate constant (in s^{-1}) of the electron injection from dye to TiO_2, k_B is the Boltzmann thermal energy, h the Planck constant, ΔG^{inject} is the free energy of injection, $-\Delta G^{inject}$ is the affinity for injection and λ is the reorganization energy of the system, $|V_{RP}|$ is the coupling constant between the reagent and the product potential curves. Eq (1) revealed that larger $|V_{RP}|$ leads to higher rate constant which would result better sensitizer. The use of the Generalized Mulliken-Hush formalism (GMH) allows evaluating $|V_{RP}|$ for a photoinduced charge transfer [41,42]. *Hsu et al.* explained that $|V_{RP}|$ can be evaluated as [42]

$$|V_{RP}| = \Delta E_{RP}/2 \quad (2)$$

The injection driving force can be formally expressed within Koopmans approximation as

$$\Delta E_{RP} = \left[E^{dye}_{LUMO} + 2E^{dye}_{HOMO}\right] - \left[E^{dye}_{LUMO} + E^{dye}_{HOMO} + E^{TiO_2}_{CBO}\right] \quad (3)$$

Archive of SID

www.SID.ir

Where $E_{CBO}^{TiO_2}$ is the conduction band edge. It is difficult to accurately determine $E_{CBO}^{TiO_2}$, because it is highly sensitive to the conditions (e.g. the pH of the solution) thus we have used $E_{CBO}^{TiO_2}$ = -4.0 eV [44] which is experimental value corresponding to conditions where the semiconductor is in contact with aqueous redox electrolytes of fixed pH 7.0 [45,46].

More quantitatively for a closed-shell system E_{LUMO}^{dye} corresponds to the reduction potential of the dye $\left(E_{RED}^{dye}\right)$, whereas the HOMO energy is related to the potential of first oxidation (i. e., - $E_{HOMO}^{dye} = E_{OX}^{dye}$). As a result, Eq. (3) becomes,

$$\Delta E_{PR} = \left[E_{OX}^{dye} + E_{OX}^{TiO_2} \right] \quad (4)$$

The eq (4) can be rewritten as

$$\Delta E_{PR} = E_{0-0}^{dye} - \left[2E_{CB}^{TiO_2} + E_{RED}^{dye} + E_{CB}^{TiO_2} \right] \quad (5)$$

The free energy change (eV) for the electron injection can be expressed as, [45]

$$\Delta G^{inject} = E_{OX}^{dye*} - E_{CB}^{TiO_2} \quad (6)$$

Where E_{OX}^{dye*} is the oxidation potential of the dye in the excited state, and $E_{CB}^{TiO_2}$ is the reduction potential of the semiconductor conduction band. Two models can be used for the evaluation of E_{OX}^{dye*} [47]. The first implies that the electron injection occurs from the unrelaxed excited state. For this reaction path, the excited state oxidation potential can be extracted from the redox potential of the ground state, E_{OX}^{dye} which has been calculated at the PCM-B3LYP-6-31G** approach and the vertical transition energy corresponding to the photoinduced intramolecular CT (ICT),

$$E_{OX}^{dye*} = E_{OX}^{dye} - \lambda_{max}^{ICT} \quad (7)$$

Where λ_{max}^{ICT} is the energy of the ICT. Note that this relation is only valid if the entropy change during the light absorption process can be neglected. For the second model, one assumes that electron injection occurs after relaxation. Given this condition, E_{OX}^{dye*} is expressed as [48]:

$$E_{OX}^{dye*} = E_{OX}^{dye} - E_{0-0}^{dye} \quad (8)$$

Where E_{0-0}^{dye} is the 0-0 transition energy between the ground state and the excited state. To estimate the 0-0 "absorption" line, we need both the S_0 (singlet ground state) and the S_1 (first singlet excited state) equilibrium geometries, Q_{S0} and Q_{S1} , respectively:

$$E_{0\text{-}0} = E_{S0}(Q_{S0}) - E_{S1}(Q_{S1}) \quad (9)$$

The absolute difference between the relaxed and unrelaxed ΔG^{inject} is constant and is of the same order of magnitude than the E_{OX}^{dye} and E_{OX}^{dye*} [45]. Here, ΔG^{inject} and E_{OX}^{dye*} have been evaluated using Eqs. (6) and (7).

The Light Harvesting Efficiency (LHE) of the dye has to be as high as possible to maximize the photocurrent response. Here, LHE is expressed as [49].

$$LHE=1\text{-}10^{-A} =1\text{-}10^{-f}$$

Where A (f) is the absorption (oscillator strength) of the dye associated to the λ_{max}^{ICT}. The oscillator strength is directly derived from the TDDFT calculations and writes:

$$f = \frac{2}{3}\lambda_{max}^{ICT} \left| \vec{\mu}_0 - ICT \right|^2$$

Where $\vec{\mu}_0 - ICT$ is the dipolar transition moment associated to the electronic excitation. In order to maximize f, both λ_{max}^{ICT} and $\vec{\mu}_0 - ICT$ must be large [50,51].

We have presented the λ_a, ΔG^{inject}, E_{OX}^{dye}, E_{OX}^{dye*}, λ_{max}^{ICT}, relative LHE (RLHE), and ΔG_r^{inject} in Table 1. The ΔG^{inject} of TC4 is -2.11, by increasing the one benzene ring between TPA and acceptor moieties (**1a**) it boosts up to -2.53. The substitution of mono-methyl (**1b**) improves the electron injection to -2.63. By increasing the two benzene rings between TPA and acceptor moieties (**2a**) enhanced the ΔG^{inject} to -2.71. The substitution of mono-methyl (**2b**) enhances the electron injection to -2.78. Three benzene rings between TPA and acceptor moieties advance the ΔG^{inject} to -2.76 (**3a**) and mono-methyl (**3b**) enhance the electron injection to -2.83. We have also observed that substitution of di- and tri-methyl (**c** and **d** derivatives) diminishes the ΔG^{inject} to some extent compared to mono-methyl (**b** derivatives). On other hand di- and tri-methyl substituted sensitizers have higher

Archive of SID

www.SID.ir

ΔG^{inject} than vinyl substituted ones. The ΔG^{inject} of new designed photosensitizers is superior to TC4. The trend of the ΔG_r^{inject} has been observed as **3** > **2** > **1** > TC4 (**b** > **c** > **d** > **a**) except **3d** which revealed that new designed photosensitizers would be efficient. In TC4, the electronic coupling constant $|V_{RP}|$ is 1.055 which improved to 1.265 by increasing the one benzene ring between TPA moiety and acceptor unit (**1a**). The $|V_{RP}|$ reaches up to 1.315, 1.300 and 1.290 in the same sensitizer by substitution of mono-, di- and tri-methyl. By increasing the two benzene rings between TPA and acceptor moieties (**2a**) the $|V_{RP}|$ boost up to 1.355 which enhanced to 1.390 by substitution of mono-methyl to improve the donor ability. It can be seen from Table 1 that by increasing the three benzene rings between TPA moiety and acceptor unit increase the $|V_{RP}|$ to 1.380 which further improved to 1.415 by substituting mono-methyl. Generally, the $|V_{RP}|$ of new designed sensitizers are higher than TC4. The improved ΔG^{inject}, ΔG_r^{inject}, and $|V_{RP}|$ than TC4 is due to the reason that (1) methyl substitution at vinyl hydrogen at position 3 and 3` is more electron donor which are favorable to promote the electron injection and electronic coupling constant. (2) Enhanced bridge is encouraging to promote the electron injection and electronic coupling constant.

The light harvesting efficiency of TC4 has been observed 0.9827. By increasing the one benzene ring between TPA moiety and anchoring group as bridge improve the LHE to 0.9934. Two benzene rings between TPA moiety and anchoring group leads improve the LHE to 0.9957. By further elongating the bridge (three benzene rings) enhances the LHE to 0.9962. The donor group has no significant effect to improve the LHE. It can be seen from Fig. 2 that by elongating the bridge efficiency enhanced.

CONCLUSIONS

The PCM-TD-B3LYP provides absorption wavelengths that are 101 nm too large compared to experimental data. The PCM-TD-LC-BLYP/6-31G** level better reproduce the experimental absorption wavelengths. The absorption spectra of new designed sensitizers are 25-34 nm blue shifted. In TC4, the maximum transition for first state is caused by HOMO ->LUMO while for new designed sensitizers it is caused by HOMO-1 -> LUMO. By increasing the benzene rings between TPA and acceptor moieties electron injection boost up. The substitution of di- and tri-methyl (**c** and **d** derivatives) diminishes the electron injection compared to mono-methyl (**b** derivatives). On other hand di- and tri-methyl substituted sensitizers have higher ΔG^{inject} than vinyl substituted ones. The electron injection of new designed photosensitizers is superior to TC4. The electronic coupling constant also improved to by increasing the benzene rings between TPA moiety and acceptor unit. The improved ΔG^{inject}, ΔG_r^{inject}, and $|V_{RP}|$ than TC4 is due to the reason that (1) methyl substitution at vinyl hydrogen at position 3 and 3` is more electron donor which are favorable to promote the electron injection and electronic coupling constant. (2) Enhanced bridge is encouraging to promote the electron injection and electronic coupling constant. Light harvesting efficiency improved by elongating. The donor group has no significant effect to improve the LHE.

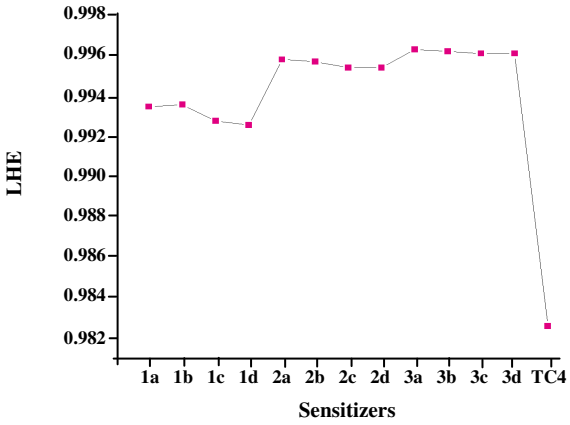

Fig. 2: The light harvesting efficiency of investigated sensitizers (LHE along Y-axis and sensitizers along X-axis).

Acknowledgement

Authors are thankful to King Khalid University support and their facility to carry out the research work.

Received : March 21, 2013 ; Accepted : Jan. 28, 2014

REFERENCES

[1] O'Regan B., Gratzel M., A Low-Cost, High-Efficiency Solar Cell Based on Dye-Sensitized Colloidal TiO_2 Films, *Nature*, **353**: 737-740 (1991).

Archive of SID
www.SID.ir

[2] Nazeeruddin Md. K., Kay A., Rodicio I., Humphrey-Baker R., Muller E., Liska P., Vlachopoulos N., Gratzel M., Conversion of Light to Electricity by Cis-X2bis (2,2′-bipyridyl-4,4′-dicarboxylate) Ruthenium(II) Charge Transfer Sensitizer (X) Cl-, Br-, I-, CN-, and SCN-) on Nanocrystalline TiO_2 Electrodes, *J Am Chem Soc*, **115**: 6382-6390 (1993).

[3] Hara K., Sayama K., Ohga Y., Shinpo A., Sugab S., Arakawa H., A Coumarin-Derivative Dye Sensitized Nanocrystalline TiO_2 Solar Cell Having a High Solar-Energy Conversion Efficiency up to 5.6%, *Chem Commun*, **6**: 569-570 (2001).

[4] Chen Z.G., Li F.Y., Huang C.H,. Organic D-π-A Dyes for Dye-Sensitized Solar Cell, *Curr Org Chem*, **11**: 1241-1258 (2007).

[5] Liu D., Fessenden R.W., Hug G.L., Kamat P.V., Dye Capped Semiconductor Nanoclusters. Role of Back Electron Transfer in the Photosensitization of SnO_2 Nanocrystallites with Cresyl Violet Aggregates, *J Phys Chem B*, **101**: 2583-2590 (1997).

[6] Li G., Jiang K.J., Li Y.F., Li S.L., Yang L.M., Efficient Structural Modification of Triphenylamine-Based Organic Dyes for Dye-Sensitized Solar Cells, *J Phys Chem C*, **112**: 11591-11599 (2008).

[7] Nazeeruddin M.K., De Angelis F., Fantacci S., Selloni A., Viscardi G., Liska P., Ito S., Bessho T., Combined Experimental and DFT-TDDFT Computational Study of Photoelectrochemical Cell Ruthenium Sensitizers, *J Am Chem Soc.*, **127**: 16835-16847 (2005).

[8] Wang S.Z., Cui Y., Hara K., Dan-Oh Y., Kasada C., Shinpo A., A High-Light-Harvesting-Efficiency Coumarin Dye for Stable Dye-Sensitized Solar Cells, *Adv Mater*, **19**: 1138-1141 (2007).

[9] Sayama K., Hara K., Mori N., Satsuki M., Suga S., Tsukagochi S., Abe Y., Sugihara H., Arakawa H., Photosensitization of a Porous TiO_2 Electrode with Merocyanine Dyes Containing a Carboxyl Group and a Long Alkyl Chain, *Chem Commun*, 1173-1174 (2000).

[10] Horiuchi T., Miura H., Sumioka K., Uchida SHigh Efficiency of Dye-Sensitized Solar Cells Based on Metal-Free Indoline Dyes, *J Am Chem Soc*, **126**: 12218-12219 (2004).

[11] Hara, K.; Horiguchi, T.; Kinoshita, T.; Sayama, K.; Sugihara, H.; Arakawa, H., Highly Efficient Photon-to-Electron Conversion with Mercurochrome-Sensitized Nanoporous Oxide Semiconductor Solar Cells, *Sol Energy Mater Sol Cells*, **64**: 115-134 (2000).

[12] Stathatos E., Lianos P., Laschewsky A., Ouari O., Van Cleuvenbergen P., Synthesis of a Hemicyanine Dye Bearing Two Carboxylic Groups and Its Use as a Photosensitizer in Dye-Sensitized Photoelectrochemical Cells, *Chem Mater*, **13**: 3888-3892 (2001).

[13] Chen R., Yang X., Tian H., Wang X., Hagfeldt A., Sun L., Effect of Tetrahydroquinoline Dyes Structure on the Performance of Organic Dye-Sensitized Solar Cells, *Chem Mater*, **19**: 4007-4015 (2007).

[14] Baik C., Kim D., Kang M.S., Song K., Sang O.K., Ko J., Synthesis and Photovoltaic Properties of Novel Organic Sensitizers Containing Indolo[1,2-f] Phenanthridine for Solar Cell, *Tetrahedron*, **65**: 5302-5307 (2009).

[15] Ferrere S., Zaban A., Gregg B., Dye Sensitization of Nanocrystalline Tin Oxide by Perylene Derivatives, *J Phys Chem B*, **101**: 4490-4493 (1997).

[16] Ferrere S., Gregg B., New Perylenes for Dye Sensitization of TiO_2, *New J Chem*, **26**: 1155-1160 (1997).

[17] Xu W., Peng B., Chen J., Liang M., Cai F., New Triphenylamine-Based Dyes for Dye-Sensitized Solar Cells, *J Phys Chem C*, 1**12**: 874-880 (2008).
(b) Irfan A., Al-Sehemi A.G., Asiri A.M., *J Mol Model*, DOI 10.1007/s00894-012-1372-9 (2012).

[18] Frisch M.J., Trucks G.W., Schlegel H.B. et al., "Gaussian 09", Revision A.1; Gaussian, Inc.: Wallingford, CT (2009).

[19] Politzer P., Abu-Awwad F., Some Approximate Kohn-Sham Molecular Energy Formulas, *Mol Phys*, **95**: 681-688 (1998).

[20] Abu-Awwad F., Politzer P., Variation of Parameters in Becke-3 Hybrid Exchange-Correlation Functional, *J Comput Chem*, **21**: 227-238 (2000).

[21] Preat J., Jacquemi D., Perpete E.A., Design of New Triphenylamine-Sensitized Solar Cells: A Theoretical Approach, *Environ Sci Technol*, **44**: 5666–5671 (2010).

Archive of SID

www.SID.ir

[22] Preat J., Michaux C., Jacquemin D., Perpe`te E.A., Enhanced Efficiency of Organic Dye-Sensitized Solar Cells: Triphenylamine Derivatives, *J Phys Chem C*, **113**: 16821–16833 (2009).

[23] Becke A.D., A New Mixing of Hartree-Fock and Local Density-Functional Theories, *J Chem Phys* **98**: 1372-1377 (1993).

[24] Becke A.D., Density-Functional Exchange-Energy Approximation with Correct Asymptotic Behavior, *Phys Rev A*, **38**: 3098-3100 (1988).

[25] Lee C., Yang W., Parr R.G., Development of the Colle-Salvetti Correlation-Energy Formula Into a Functional of the Electron Density, *Phys Rev B*, **37**: 785-789 (1988).

[26] Krishnan R., Binkley J.S., Seeger R., Pople J.A., Self-Consistent Molecular Orbital Methods. XX. A Basis Set for Correlated Wave Functions, *J Chem Phys*, **72**: 650-655 (1980).

[27] Stein T., Kronik L., Baer R., Prediction of Charge-Transfer Excitations in Coumarin-Based Dyes using a Range-Separated Functional Tuned from First Principles, *J Chem Phys*, **131**: 244119-244123 (2009).

[28] Wong B.M., Piacenza M., Sala F.D., Absorption and Fluorescence Properties of Oligothiophene Biomarkers from Long-Range-Corrected Time-Dependent Density Functional Theory, *Phys Chem Chem Phys*, **11**: 4498-4508 (2009).

[29] Wong B.M., Cordaro J.G., Coumarin Dyes for Dye-Sensitized Solar Cells: A Long-Range-Corrected Density Functional Study, *J Chem Phys*, **129**: 214703-214710 (2008).

[30] Lange A.W., Rohrdanz M.A., Herbert J.M., Charge-Transfer Excited States in a π-Stacked Adenine Dimer, as Predicted using Long-Range-Corrected Time-Dependent Density Functional Theory, *J Phys Chem B*, **112**: 6304-6308 (2008).

[31] Rohrdanz M.A., Herbert J.M., Simultaneous Benchmarking of Ground- and Excited-State Properties with Long-Range-Corrected Density Functional Theory. *J Chem Phys*, **129**: 034107-034115 (2008).

[32] Toulouse J., Colonna F., Savin A., Short-Range Exchange and Correlation Energy Density Functionals: Beyond the Local-Density Approximation, *J Chem Phys*, **122**: 014110-014119 (2005).

[33] Livshits E., Baer R., A Well-Tempered Density Functional Theory of Electrons in Molecules, *Phys Chem Chem Phys*, **9**: 2932-2941 (2007).

[34] Irfan A., Cui R., Zhang J., Hao L., Push-Pull Effect on the Charge Transfer, and Tuning of Emitting Color for Disubstituted Derivatives of Mer-Alq3, *Chem Phys*, **364**: 39-45 (2009).

(b) Irfan A., Al-Sehemi A.G., Muhammad, S., Push-Pull Effect on the Charge Transport Properties in Anthra[2,3-b]Thiophene Derivatives Used as Dye-Sensitized and Hetero-Junction Solar Cell Materials, *Synth Met,* **190**: 27-33 (2014).

(c) Irfan A., Al-Sehemi A.G., Al-Assiri M.S., Push–Pull Efect on the Electronic, Optical and Ccharge Transport Properties of the Bbenzo[2,3-b] Thiophene Derivatives as Efficient Multifunctional Materials, *Comp Theor Chem*, **1031**: 76-82 (2014).

(d) Irfan A., Al-Sehemi A.G., Al-Assiri M.S., The Effect of Donors-Acceptors on the Charge Transfer Properties and Tuning of Emitting Color for Thiophene, Pyrimidine and Oligoacene Based Compounds, *J Fluorine Chem*, **157**: 52-57 (2014).

(e) Irfan A., Highly Efficient Renewable Energy Materials Benzo[2,3-b]Thiophene Derivatives: Electronic and Charge Transfer Properties Study, *Optik - Inter J Light Elect Optics* **125**: 4825-4830 (2014).

(f) Irfan, A., First Principle Investigations to Enhance the Charge Transfer Properties by Bridge Elongation, *J Theor Comput Chem*, **13**: 1450013-1450024 (2014).

(g) Irfan A., Modeling of Efficient Charge Transfer Materials of 4,6-di(Thiophen-2-yl)Pyrimidine Derivatives: Quantum Chemical Investigations, *Comp Mater Sci* **81**: 488-492 (2014).

(h) Irfan, A., Jin, R., Al-Sehemi, A.G., Asiri, A.M., Quantum Chemical Study of the Donor-Bridge-Acceptor Triphenylamine Based Sensitizers, *Spectrochimica Acta Part A: Molecular and Biomolecular Spectroscopy* **110**: 60-66 (2013).

(i) Irfan A., Al-Sehemi A.G., Kalam A., Structural, Electronic and Charge Transfer Studies of Dianthra[2,3-b:2′,3′-f]Thieno[3,2-b]Thiophene and Its Analogues: Quantum Chemical Investigations, *J Mol Struct*, **1049**: 198-204 (2013).

(j) Irfan A., Al-Sehemi A.G., Al-Assiri M.S., Modeling of Multifunctional Donor-Bridge-Acceptor 4,6-Di(Thiophen-2-yl)Pyrimidine Derivatives: A First Principles Study, *J Mol Graphics Modell*, **44**: 168-176 (2013).

Archive of SID

www.SID.ir

(k) Irfan A., Quantum Chemical Investigations of Electron Injection in Triphenylamine-Dye Sensitized TiO_2 Used in Dye Sensitized Solar Cells, *Mater Chem Phys*, **142**: 238-247 (2013).

(l) Chaudhry, A.R., Ahmed, R., Irfan, A., Muhammad, S., Shaari, A., Al-Sehemi, A.G., Effect of Heteroatoms Substitution on Electronic, Photophysical and Charge Transfer Properties of Naphtha [2,1-b:6,5-b′] Difuran Analogues by Density Functional Theory, *Comp Theor Chem*, **1045**: 123-134 (2014).

[35] Sun J., Song J., Zhao Y., Liang W.Z., Real-Time Propagation of the Reduced One-Electron Density Matrix in Atom-Centered Gaussian Orbitals: Application to Absorption Spectra of Silicon Clusters, *J Chem Phys*, **127**: 234107-234113 (2007).

[36] Zhang C.R., Liang W.Z., Chen H.S., Chen Y.H., Wei Z.Q., Wu Y.Z., Theoretical Studies on the Geometrical and Electronic Structures of N-Methyle-3,4-Fulleropyrrolidine. *J Mol Struct (THEOCHEM)*, **862**: 98-104 (2008).

[37] Cossi M., Barone V., Time-Dependent Density Functional Theory for Molecules in Liquid Solutions, *J Chem Phys*, **115**: 4708-4717 (2001).

[38] Amovilli C., Barone V., Cammi R., Cancès E., Cossi M., Mennucci B., Pomelli C.S., Tomasi J., Recent Advances in the Description of Solvent Effects with the Polarizable Continuum Model, *Adv Quant Chem*, **32**: 227-262 (1998).

[39] Tomasi J., Mennucci B., Cammi R., Quantum Mechanical Continuum Solvation Models, *Chem Rev*, **105**: 2999-3094 (2005).

[40] Preat J., Jacquemin D., Perpete E., Design of New Triphenylamine-Sensitized Solar Cells: A Theoretical Approach, *Environ Sci Technol*, **44**: 5666–5671 (2010).

[41] Pourtois G., Beljonne J., Ratner M.A., Bredas J.L., Photoinduced Electron-Transfer Processes Along Molecular Wires Based on Phenylenevinylene Oligomers: A Quantum-Chemical Insight, *J Am Chem Soc*, **124**: 4436-4447 (2002).

[42] Hsu C., The Electronic Couplings in Electron Transfer and Excitation Energy Transfer, *Acc Chem Res*, **42**: 509-518 (2009).

[43] Marcus R.A., Electron Transfer Reactions in Chemistry. Theory and Experiment, *Rev Mod Phys*, **65**: 599-610 (1993).

[44] Asbury J.B., Wang Y.Q., Hao E., Ghosh H., Lian T., Evidences of Hot Excited State Electron Injection from Sensitizer Molecules to TiO_2 Nanocrystalline Thin Films, *Res Chem Intermed*, **27**: 393-406 (2001).

[45] Katoh R., Furube A., Yoshihara T., Hara K. et al., Efficiencies of Electron Injection from Excited N3 Dye Into Nanocrystalline Semiconductor (ZrO_2, TiO_2, ZnO, Nb_2O_5, SnO_2, In_2O_3) Films, *J Phys Chem B*, **108**: 4818-4822 (2004).

[46] Hagfeldt A., Grätzel M., Light-Induced Redox Reactions in Nanocrystalline Systems, *Chem Rev*, **95**: 49-68 (1995).

[47] Barbara P.F., Meyer T.J., Ratner M.A., Contemporary Issues in Electron Transfer Research, *J Phys Chem*, **100**: 13148-13168 (1996).

[48] De Angelis F., Fntacci S., Selloni A., Alignment of the Dye's Molecular Levels with the TiO_2 Band Edges in Dye-Sensitized Solar Cells: a DFT–TDDFT Study, *Nanotechnology*, **19**: 424002-424009 (2008).

[49] Nalwa H.S., "Handbook of Advanced Electronic and Photonic Materials and Devices", Academic: San Diego CA (2001).

[50] Cassida M., "Recent Advances in Density Functional Methods: Time Dependent Density Functional Response Theory for Molecules", DP Chong: Singapore (1995)

[51] Harris D.C., Bertolucci M.D, "Symmetry and Spectroscopy", Dover: New York US (1998).

Archive of SID

www.SID.ir

Appendix

Absorption spectrum of TC4 at PCM-TD-B3LYP/6-31G** level of theory and %age contribution

No.	Energy (cm-1)	Wavelength (nm)	Osc. Strength	Major contribs Minor contribs
1	19005.77984	526.15	1.0987	HOMO->LUMO (99%)
2	27526.27968	363.29	0.4872	H-1->LUMO (81%), HOMO->L+1 (16%)
3	29405.56448	340.07	0.1827	H-1->LUMO (15%), HOMO->L+1 (79%), HOMO->L+3 (2%)
4	30657.3456	326.19	0.2124	H-2->LUMO (78%), H-5->LUMO (3%), H-4->LUMO (7%), HOMO->L+2 (3%), HOMO->L+3 (6%)
5	31377.60368	318.69	0.0185	H-4->LUMO (21%), H-2->LUMO (12%), HOMO->L+2 (52%)H-5->LUMO (7%), H-3->LUMO (5%)
6	32089.79616	311.62	0.0159	H-3->LUMO (90%), HOMO->L+2 (6%)
7	32745.52944	305.38	0.0875	H-5->LUMO (12%), H-4->LUMO (43%), HOMO->L+2 (30%), HOMO->L+3 (8%)
8	33685.17184	296.86	0.0071	H-5->LUMO (63%), H-4->LUMO (22%), HOMO->L+3 (4%), HOMO->L+4 (8%)
9	33840.83792	295.50	0.0863	HOMO->L+3 (73%), H-6->LUMO (2%), H-5->LUMO (2%), H-4->LUMO (6%), H-2->LUMO (5%), HOMO->L+2 (3%)
10	34876.46096	286.72	0.0001	H-7->LUMO (96%)

Absorption spectrum of TC4 at PCM-TD-LC-BLYP/6-31G** level of theory and %age contribution

No.	Energy (cm-1)	Wavelength (nm)	Osc. Strength	Major contribs Minor contribs
1	26830.2184	372.71	1.7622	H-1->LUMO (18%), HOMO->LUMO (70%), HOMO->L+3 (3%)
2	37029.97616	270.05	0.2181	H-1->LUMO (11%), HOMO->L+1 (62%) H-1->L+1(9%)
3	38827.7984	257.54	0.003	HOMO->L+2 (34%), HOMO->L+3 (14%) H-5->LUMO (9%), H-4->LUMO (9%), H-1->LUMO (6%), H-1->L+4 (3%), HOMO->L+4 (4%)
4	39556.12208	252.80	0.4407	H-2->LUMO (12%), H-1->LUMO (17%), HOMO->L+2 (15%), HOMO->L+3 (22%) H-6->LUMO (6%), H-2->L+3 (2%), H-1->L+1 (3%), HOMO->LUMO (4%), HOMO->L+1 (7%)
5	41230.54064	242.54	0.0058	HOMO->L+4 (30%) H-5->LUMO (9%), H-5->L+1(4%), H-4->L+1 (7%), H-3- >L+1 (7%), H-2->L+5 (2%), H-1->L+2 (9%), H-1->L+5 (4%), HOMO->L+2 (6%), HOMO->L+5 (3%)
6	43176.76992	231.61	0.0085	H-2->L+2 (10%), HOMO->L+5 (32%) H-6->L+2 (2%), H-6->L+5 (3%), H-5->LUMO (2%), H-5->L+3 (3%), H-4->L+1 (5%), H-3->L+3 (8%), H-3->L+6 (6%), H-2->L+4 (3%), H-2->L+5 (8%), H-1->L+5 (3%), HOMO->L+2 (4%)
7	44415.64608	225.14	0.0002	H-8->LUMO (55%), H-8->L+7 (23%) H-8->L+3 (9%), H-8->L+6 (5%)
8	45758.56848	218.54	0.1898	HOMO->L+3 (23%), HOMO->L+6 (12%) H-6->LUMO (6%), H-4->LUMO (3%), H-2->LUMO (3%), H-2->L+1 (6%), H-2->L+3 (3%), H-1->LUMO (5%), H-1->L+1 (5%), HOMO->LUMO (9%), HOMO->L+4 (6%)
9	47137.78608	212.14	0.2381	H-5->LUMO (18%), H-4->LUMO (14%), HOMO->L+2 (15%) H-4->L+1 (2%), H-2->LUMO (2%), H-1->LUMO (4%), H-1->L+1 (5%), HOMO->LUMO (4%), HOMO->L+1 (3%), HOMO->L+3 (4%), HOMO->L+4 (9%)
10	48161.31072	207.63	0.0192	H-2->L+1 (11%), H-1->LUMO (10%), H-1->L+1 (11%), HOMO->L+6 (10%) H-5->LUMO (4%), H-4->LUMO (4%), H-3->L+1 (2%), H-2->LUMO (3%), H-1->L+3 (6%), HOMO->LUMO (4%), HOMO->L+1 (4%), HOMO- >L+2 (4%), HOMO->L+3 (7%)

Archive of SID

www.SID.ir

Absorption spectrum of 1a at PCM-TD-LC-BLYP/6-31G** level of theory and %age contribution

No.	Energy (cm-1)	Wavelength (nm)	Osc. Strength	Major contribs Minor contribs
1	28760.31648	347.70	2.1805	H-1->LUMO (55%), HOMO->LUMO (27%), H-3->LUMO (4%), HOMO->L+2 (6%)
2	35191.01936	284.16	0.8866	HOMO->L+1 (77%) H-2->L+2 (4%), H-2->L+3 (2%), H-2->L+4 (2%), H-1->L+1 (6%), HOMO->L+11 (3%)
3	35428.148	282.26	0.1577	H-3->LUMO (10%), H-1->LUMO (15%), HOMO->L+2 (48%) H-2->L+1 (3%), HOMO->LUMO (8%), HOMO->L+8 (4%)
4	38498.72192	259.75	0.0121	HOMO->L+3 (46%), HOMO->L+4 (20%) H-5->L+2(3%), H-4->L+1 (3%), H-3->L+6 (3%), H-2->L+7 (6%), H-1->L+6 (2%
5	40172.33392	248.93	0.0092	H-6->LUMO (51%), H-1->L+5 (15%),H-8->L+5 (2%), H-6->L+2 (5%), H-6->L+3 (3%), H-6->L+4 (4%), H-6->L+8 (3%), HOMO->L+5 (7%)
6	41332.1672	241.94	0.0295	HOMO->L+6 (35%) H-7->L+2 (7%), H-3->L+3 (4%), H-3->L+6 (2%), H-2->L+7 (4%), H-1->L+3 (3%), HOMO->LUMO (2%), HOMO->L+4 (5%), HOMO->L+5 (3%)
7	41587.84672	240.45	0.0153	HOMO->L+7 (43%) H-7->L+1 (8%), H-5->L+1 (4%), H-4->L+1 (3%), H-4->L+2 (3%), H-4->L+4 (2%), H-2->L+3 (8%), H-2->L+4 (3%), H-2->L+6 (4%), H-1->L+7 (5%)
8	42150.8256	237.24	0.1741	H-3->LUMO (11%), HOMO->LUMO (20%), HOMO->L+4 (15%), H-8->LUMO (5%), H-2->L+1 (9%), H-1->L+2 (5%), HOMO->L+2 (7%), HOMO->L+3 (4%), HOMO->L+6 (6%)
9	45831.15888	218.19	0.0233	H-1->L+2 (21%), HOMO->LUMO (34%) H-8->LUMO (3%), H-2->L+1 (3%), H-1->LUMO (7%), H-1->L+3 (3%), H-1->L+4 (2%), HOMO->L+2 (7%), HOMO->L+8 (2%)
10	46423.98048	215.40	0.0444	H-8->LUMO (17%), H-2->L+1 (17%), HOMO->L+8 (13%), H-9->LUMO (6%), H-6->L+5 (2%), H-3->LUMO (5%), H-3->L+2 (6%), H-1->L+3 (4%), H-1->L+4 (5%), HOMO->L+4 (2%)

Absorption spectrum of 1b at PCM-TD-LC-BLYP/6-31G** level of theory and %age contribution

No.	Energy (cm-1)	Wavelength (nm)	Osc. Strength	Major contribs Minor contribs
1	28636.9128	349.20	2.1873	H-1->LUMO (53%), HOMO->LUMO (26%), H-3->LUMO (6%), HOMO->L+1 (6%)
2	35312.80992	283.18	0.3744	H-1->LUMO (12%), HOMO->L+1 (51%) H-3->LUMO (9%), HOMO->LUMO (7%), HOMO->L+8 (3%)
3	35801.58528	279.32	0.7395	HOMO->L+2 (70%) H-3->LUMO (2%), H-2->L+4 (4%), H-1->LUMO (2%), H-1->L+2 (2%), HOMO->LUMO (2%), HOMO->L+11 (2%)
4	38383.38384	260.53	0.0139	HOMO->L+3 (60%) H-5->L+1 (4%), H-4->L+2 (4%), H-3->L+6 (2%), H-2->L+7 (4%), HOMO->L+4 (6%)
5	40152.16992	249.05	0.0094	H-6->LUMO (47%), H-1->L+5 (14%), H-7->LUMO (5%), H-6->L+1 (5%), H-6->L+4 (5%), H-6->L+8 (2%), H-1->L+3 (2%), HOMO->L+5 (7%)
6	41299.9048	242.13	0.0472	HOMO->L+6 (18%), HOMO->L+7 (21%) H-7->LUMO (2%), H-7->L+1 (7%), H-5->L+2 (3%), H-5->L+8 (2%), H-4->L+1 (3%), H-3->L+3 (4%), H-3->L+6 (2%), H-2->L+7 (4%), H-1->L+3 (5%), HOMO->L+4 (3%), HOMO->L+5 (3%)
7	41516.06288	240.87	0.0187	HOMO->L+6 (24%), HOMO->L+7 (20%) H-7->L+2(6%), H-5->L+1 (3%), H-5->L+2 (3%), H-4->L+2 (3%), H-4->L+4 (4%), H-2->L+3 (9%), H-2->L+6 (6%), H-1->L+7 (3%)
8	42085.49424	237.61	0.2029	H-3->LUMO (11%), HOMO->LUMO (23%), HOMO->L+4 (20%)H-8->LUMO (6%), H-2->L+2 (8%), H-1->L+1 (4%), HOMO->L+1 (6%), HOMO->L+7 (3%)
9	45564.99408	219.47	0.0335	H-1->L+1 (20%), HOMO->LUMO (32%) H-8->LUMO (3%), H-2->L+2 (4%), H-1->LUMO (7%), H-1->L+2 (3%), HOMO->L+1 (6%), HOMO->L+4 (3%), HOMO->L+8 (3%)
10	46411.07552	215.46	0.0487	H-8->LUMO (15%), H-2->L+2 (12%), HOMO->L+8(12%), H-10->LUMO (2%), H-9->LUMO (7%), H-3->LUMO (4%), H-3->L+1 (7%), H-2->L+1 (6%), H-1->L+4 (8%)

Archive of SID

www.SID.ir

Absorption spectrum of 1c at PCM-TD-LC-BLYP/6-31G** level of theory and %age contribution

No.	Energy (cm-1)	Wavelength (nm)	Osc. Strength	Major contribs Minor contribs
1	28645.78496	349.09	2.1371	H-1->LUMO (51%), HOMO->LUMO (28%), H-3->LUMO (5%), HOMO->L+1 (6%)
2	35733.02768	279.85	0.169	H-3->LUMO (10%), H-1->LUMO (13%), HOMO->L+1 (44%), H-8->LUMO (4%), HOMO->LUMO (9%), HOMO->L+4 (2%), HOMO->L+5 (2%), HOMO->L+8 (3%)
3	37430.83648	267.15	0.7817	HOMO->L+2 (75%), H-2->L+5 (3%), H-1->L+2 (5%)
4	38621.31904	258.92	0.039	HOMO->L+3 (66%), H-5->L+1 (4%), H-4->L+2 (3%), H-2->L+7 (3%)
5	40153.78304	249.04	0.0071	H-7->LUMO (26%), H-6->LUMO (26%), H-10->L+4 (2%), H-7->L+1 (3%), H-7->L+5 (2%), H-6->L+1 (4%), H-1->L+4 (9%), H-1->L+5 (4%), HOMO->L+4 (6%), HOMO->L+5 (2%)
6	41517.676	240.86	0.0361	HOMO->L+6 (28%), HOMO->L+7 (16%), H-8->L+3 (3%), H-7->LUMO (3%), H-7->L+1 (5%), H-6->L+1 (3%), H-4->L+2 (6%), H-3->L+3 (3%), H-2->L+7 (4%), H-1->L+3 (6%)
7	42026.61536	237.94	0.0174	HOMO->L+6 (15%), HOMO->L+7 (30%), H-9->L+3 (2%), H-7->L+2 (2%), H-6->L+2 (3%), H-5->L+2 (6%), H-4->L+1 (3%), H-4->L+5 (3%), H-2->L+3 (9%), H-2->L+6 (5%), H-1->L+7 (4%)
8	42841.24096	233.42	0.1561	HOMO->LUMO (25%), HOMO->L+5 (16%), H-10->LUMO (3%), H-8->LUMO (9%), H-3->LUMO (8%), H-2->L+2 (6%), H-1->L+1 (4%), HOMO->L+1 (8%), HOMO->L+4 (9%)
9	44123.67136	226.63	0.0002	H-11->LUMO (54%), H-11->L+1 (10%), H-11->L+9 (21%), H-11->L+5 (3%), H-11->L+8 (5%)
10	45890.84432	217.91	0.04	H-1->L+1 (28%), HOMO->LUMO (28%), H-10->LUMO (6%), H-8->LUMO (5%), H-1->LUMO (8%), HOMO->L+1 (6%)

Absorption spectrum of 1d at PCM-TD-LC-BLYP/6-31G** level of theory and %age contribution

No.	Energy (cm-1)	Wavelength (nm)	Osc. Strength	Major contribs Minor contribs
1	28629.65376	349.28	2.1271	H-1->LUMO (50%), HOMO->LUMO (31%), H-3->LUMO (5%), HOMO->L+1 (6%)
2	35970.15632	278.01	0.1253	H-1->LUMO (15%), HOMO->LUMO (10%), HOMO->L+1 (42%) H-6->LUMO (6%), H-3->LUMO (7%), HOMO->L+5 (6%)
3	38490.65632	259.80	0.3169	HOMO->L+2 (69%) H-1->L+2 (3%), HOMO->L+3 (5%)
4	39047.18272	256.10	0.4346	HOMO->L+3 (64%) H-5->L+1 (2%), HOMO->L+2 (8%)
5	40155.39616	249.03	0.0056	H-9->LUMO (19%), H-8->LUMO (23%), H-7->LUMO (10%), H-1->L+4 (12%), H-10->L+4 (3%), H-9->L+1 (3%), H-8->L+1 (4%), H-8->L+5 (2%), HOMO->L+4 (8%)
6	41740.28656	239.57	0.0415	HOMO->L+6 (44%), H-9->L+1 (2%), H-7->L+1 (5%), H-6->L+3 (5%), H-4->L+2 (7%), H-2->L+7 (3%), H-1->L+2 (2%), H-1->L+3 (4%), HOMO->L+4 (4%)
7	42413.76416	235.77	0.0116	HOMO->L+7 (45%), H-8->L+2 (4%), H-7->L+2 (4%), H-6->L+7 (2%), H-5->L+2 (3%), H-5->L+3 (5%), H-4->L+5 (4%), H-2->L+3 (5%), H-2->L+6 (2%), H-1->L+7 (6%)
8	43330.01632	230.78	0.1548	H-6->LUMO (12%), HOMO->LUMO (25%), HOMO->L+5 (21%), H-10->LUMO (6%), H-3->LUMO (4%), H-1->L+1 (3%), HOMO->L+1 (9%), HOMO->L+4 (3%)
9	44126.8976	226.61	0.0002	H-11->LUMO (55%), H-11->L+1 (11%), H-11->L+9 (19%), H-11->L+5 (5%), H-11->L+8 (6%)
10	46121.52048	216.81	0.0412	H-1->L+1 (29%), HOMO->LUMO (25%), H-10->LUMO (9%), H-6->LUMO (5%), H-1->LUMO (9%), H-1->L+5 (2%), HOMO->L+1 (6%)

Archive of SID

www.SID.ir

Absorption spectrum of 2a at PCM-TD-LC-BLYP/6-31G** level of theory and %age contribution

No.	Energy (cm-1)	Wavelength (nm)	Osc. Strength	Major contribs Minor contribs
1	29362.01024	340.57	2.3668	H-3->LUMO (14%), H-1->LUMO (66%), HOMO->LUMO (7%), HOMO->L+1 (3%)
2	34858.71664	286.87	0.5756	HOMO->L+1 (52%), HOMO->L+3 (11%), H-3->LUMO (6%), H-3->L+1 (2%), H-2->L+2 (3%), H-1->LUMO (3%), HOMO->LUMO (4%)
3	35018.41552	285.56	0.9159	HOMO->L+2 (76%), H-2->L+3 (5%), H-1->L+2 (4%), HOMO->L+13 (3%)
4	38471.29888	259.93	0.0147	HOMO->L+4 (57%), H-5->L+1 (3%), H-4->L+2 (5%), H-3->L+8 (3%), H-2->L+9 (6%), HOMO->L+3 (9%)
5	40218.30784	248.64	0.0084	H-7->LUMO (49%), H-1->L+5 (14%), H-8->LUMO (5%), H-7->L+1 (3%), H-7->L+3 (4%), H-7->L+7 (5%), H-1->L+6 (2%), H-1->L+7 (2%)
6	40786.12608	245.18	0.0649	H-3->LUMO (13%), H-1->L+1 (19%), HOMO->L+3 (16%) H-8->LUMO (7%), H-2->L+2 (5%), HOMO->LUMO (7%), HOMO->L+4 (5%)
7	41493.4792	241.00	0.0119	HOMO->L+8 (33%) H-9->L+1 (4%), H-5->L+1 (3%), H-4->L+2 (5%), H-3->L+4 (6%), H-2->L+9 (3%), H-1->L+4 (2%), HOMO->L+6 (5%), HOMO->L+9 (2%)
8	41528.16128	240.80	0.0234	HOMO->L+9 (41%) H-9->L+2 (8%), H-5->L+2 (5%), H-4->L+1 (2%), H-4->L+3 (5%), H-2->L+4 (9%), H-2->L+8 (4%), H-1->L+9 (3%)
9	42266.97024	236.59	0.0004	H-6->LUMO (10%), H-6->L+1 (24%), H-1->L+6 (11%) H-8->L+6 (3%), H-6->L+3 (4%), H-6->L+11 (5%), H-3->L+5 (2%), H-3->L+6 (3%), H-1->L+5 (6%), H-1->L+7 (2%), HOMO->L+5 (3%), HOMO->L+6 (3%), HOMO->L+8 (5%)
10	44726.97824	223.57	0.0545	H-2->L+2 (18%), HOMO->L+7 (12%) H-10->LUMO (5%), H-8->LUMO (7%), H-3->L+1 (7%), H-1->LUMO (2%), H-1->L+3 (7%), HOMO->L+1 (2%), HOMO->L+3 (7%), HOMO->L+6 (3%), HOMO->L+11 (2%)

Absorption spectrum of 2b at PCM-TD-LC-BLYP/6-31G** level of theory and %age contribution

No.	Energy (cm-1)	Wavelength (nm)	Osc. Strength	Major contribs Minor contribs
1	29332.97408	340.91	2.3557	H-3->LUMO (15%), H-1->LUMO (65%) HOMO->LUMO (7%), HOMO->L+1 (3%)
2	34962.76288	286.01	0.5439	HOMO->L+1 (49%), HOMO->L+3 (15%) H-3->LUMO (6%), H-3->L+1 (3%), H-2->L+2 (3%), H-1->LUMO (2%), H-1->L+1 (2%), HOMO->LUMO (5%)
3	35981.44816	277.92	0.9509	HOMO->L+2 (78%) H-2->L+3 (5%), H-1->L+2 (4%), HOMO->L+13 (3%)
4	38474.52512	259.91	0.0241	HOMO->L+4 (66%) H-5->L+1 (3%), H-4->L+2 (5%), H-3->L+8 (3%), H-2->L+9 (6%)
5	40208.62912	248.70	0.0088	H-9->LUMO (54%), H-1->L+5 (14%) H-9->L+1 (4%), H-9->L+3 (6%), H-9->L+7 (5%), H-1->L+6 (3%)
6	40945.0184	244.22	0.0652	H-7->LUMO (10%), H-3->LUMO (12%), H-1->L+1 (20%), HOMO->L+3 (18%) H-10->LUMO (3%), H-2->L+2 (4%), HOMO->LUMO (7%), HOMO->L+9 (3%)
7	41444.27904	241.28	0.025	HOMO->L+8 (39%) H-10->L+4 (2%), H-8->L+1 (5%), H-8->L+3 (3%), H-5->L+1 (3%), H-5->L+7 (3%), H-4->L+2 (5%), H-3->L+4 (8%), H-3->L+8 (2%), H-2->L+9 (4%), H-1->L+4 (4%), HOMO->L+6 (5%)
8	41590.2664	240.44	0.0258	H-2->L+4 (11%), HOMO->L+9 (43%) H-11->L+4 (2%), H-8->L+2 (7%), H-5->L+2 (6%), H-4->L+3 (5%), H-2->L+8 (4%), H-1->L+9 (3%)
9	42248.41936	236.69	0.0005	H-6->LUMO (10%), H-6->L+1 (25%), H-1->L+6 (13%) H-7->L+5 (2%), H-7->L+6 (4%), H-6->L+3 (2%), H-6->L+11 (5%), H-3->L+6 (3%), H-1->L+5 (7%), HOMO->L+5 (3%), HOMO->L+6 (4%), HOMO->L+8 (6%)
10	45127.032	221.59	0.0478	H-2->L+2 (17%), HOMO->L+7 (15%) H-12->LUMO (3%), H-10->LUMO (6%), H-7->LUMO (7%), H-3->L+1 (7%), H-1->LUMO (2%), H-1->L+3 (8%), HOMO->LUMO (4%), HOMO->L+3 (6%)

Archive of SID

www.SID.ir

Absorption spectrum of 2c at PCM-TD-LC-BLYP/6-31G** level of theory and %age contribution

No.	Energy (cm-1)	Wavelength (nm)	Osc. Strength	Major contribs Minor contribs
1	29336.20032	340.87	2.3269	H-3->LUMO (13%), H-1->LUMO (65%) HOMO->LUMO (8%), HOMO->L+1 (3%)
2	35355.5576	282.84	0.5381	HOMO->L+1 (49%), HOMO->L+4 (16%) H-3->LUMO (6%), H-3->L+1 (3%), H-1->LUMO (3%), H-1->L+1 (3%), HOMO->LUMO (5%)
3	37769.59168	264.76	0.7354	HOMO->L+2 (78%) H-2->L+9 (2%), H-1->L+2 (5%), HOMO->L+13 (2%)
4	38778.59824	257.87	0.0472	HOMO->L+3 (67%) H-11->L+7 (2%), H-10->L+8 (2%), H-6->L+1 (3%), H-5->L+2 (3%), H-3->L+7 (3%), H-2->L+8 (4%)
5	40206.20944	248.71	0.0095	H-9->LUMO (54%), H-1->L+5 (12%) H-9->L+1 (4%), H-9->L+4 (7%), H-9->L+9 (3%), H-1->L+6 (5%)
6	41348.2984	241.84	0.0554	H-3->LUMO (11%), H-1->L+1 (21%), HOMO->L+4(16%) H-11->LUMO (8%), H-5->LUMO (3%), H-4->LUMO (7%), HOMO->LUMO (7%)
7	41654.7912	240.06	0.0384	HOMO->L+7 (35%) H-11->L+3 (3%), H-8->L+1 (4%), H-8->L+4 (3%), H-7->L+1 (3%), H-6->L+1 (2%), H-5->L+2 (4%), H-3->L+3 (6%), H-2->L+8 (4%), H-1->L+3 (4%), HOMO->L+5 (2%), HOMO->L+6 (6%), HOMO->L+9 (3%)
8	42177.44208	237.09	0.0267	HOMO->L+8 (44%) H-10->L+3 (4%), H-8->L+2 (7%), H-6->L+2 (5%), H-5->L+4 (3%), H-5->L+9 (2%), H-2->L+3 (8%), H-2->L+7 (3%), H-1->L+8 (4%)
9	42258.90464	236.63	0.002	-7->LUMO (10%), H-7->L+1 (25%), H-1->L+6(11%) H-7->L+9 (2%), H-7->L+11 (4%), H-4->L+6 (3%), H-3->L+6 (2%), H-1->L+5 (7%), HOMO->L+5 (3%), HOMO->L+6 (4%), HOMO->L+7 (9%)
10	44092.21552	226.79	0.0002	H-13->LUMO (54%), H-13->L+10 (24%) H-13->L+1 (8%), H-13->L+4 (6%), H-13->L+9 (3%)

Absorption spectrum of 2d at PCM-TD-LC-BLYP/6-31G** level of theory and %age contribution

No.	Energy (cm-1)	Wavelength (nm)	Osc. Strength	Major contribs Minor contribs
1	29315.22976	341.11	2.3302	H-3->LUMO (10%), H-1->LUMO (64%) H-4->LUMO (5%), HOMO->LUMO (8%), HOMO->L+1 (3%)
2	35386.20688	282.59	0.5389	HOMO->L+1 (48%), HOMO->L+4 (15%) H-4->LUMO (4%), H-3->LUMO (4%), H-3->L+1 (2%), H-1->LUMO (3%), H-1->L+1 (3%), HOMO->LUMO (5%), HOMO->L+5 (2%)
3	38469.68576	259.94	0.5051	HOMO->L+2 (74%) H-1->L+2 (4%)
4	38902.00192	257.05	0.2537	HOMO->L+3 (67%) HOMO->L+2 (4%)
5	40202.17664	248.74	0.0096	H-10->LUMO (54%), H-1->L+5 (11%) H-10->L+1 (4%), H-10->L+4 (7%), H-10->L+9 (3%), H-1->L+4 (3%), H-1->L+6 (5%)
6	41435.40688	241.33	0.054	H-11->LUMO (10%), H-4->LUMO (12%), H-1->L+1 (21%), HOMO->L+4 (14%) H-3->LUMO (6%), HOMO->LUMO (7%), HOMO->L+5 (3%), HOMO->L+9 (3%)
7	41702.37824	239.79	0.0456	HOMO->L+7 (36%) H-11->L+3 (3%), H-9->L+8 (2%), H-8->L+1 (3%), H-8->L+4 (3%), H-7->L+1 (4%), H-5->L+2 (3%), H-4->L+3 (2%), H-3->L+3 (3%), H-2->L+8 (3%), H-1->L+3 (3%), HOMO->L+5 (3%), HOMO->L+6 (7%)
8	42250.03248	236.68	0.0033	H-7->L+1 (24%), H-1->L+6 (11%), HOMO->L+7 (11%) H-7->LUMO (9%), H-7->L+9 (3%), H-7->L+11 (3%), H-4->L+5 (3%), H-4->L+6 (4%), H-1->L+5 (6%), HOMO->L+5 (3%), HOMO->L+6 (4%)
9	42365.37056	236.04	0.0267	HOMO->L+8 (45%) H-9->L+3 (4%), H-9->L+7 (2%), H-8->L+2 (7%), H-6->L+2 (3%), H-5->L+9 (2%), H-4->L+8 (2%), H-2->L+3 (6%), H-2->L+7 (2%), H-1->L+8 (5%)
10	44092.21552	226.79	0.0002	H-13->LUMO (54%), H-13->L+10 (23%) H-13->L+1 (8%), H-13->L+4 (6%), H-13->L+9 (3%)

Archive of SID

www.SID.ir

Absorption spectrum of 3a at PCM-TD-LC-BLYP/6-31G** level of theory and %age contribution

No.	Energy (cm-1)	Wavelength (nm)	Osc. Strength	Major contribs Minor contribs
1	29499.12544	338.99	2.4158	H-2->LUMO (26%), H-1->LUMO (57%) H-4->LUMO (4%)
2	34617.5552	288.87	1.1046	HOMO->L+1 (44%), HOMO->L+3 (24%) H-3->L+2 (3%), H-2->LUMO (3%), H-2->L+1 (4%), H-1->L+1 (4%), HOMO->L+11 (2%)
3	34969.21536	285.96	0.9105	HOMO->L+2 (77%) H-3->L+3 (5%), H-2->L+2 (2%), H-1->L+2 (4%), HOMO->L+15 (3%)
4	38437.42336	260.16	0.029	HOMO->L+4 (56%) H-6->L+2 (4%), H-5->L+1 (2%), H-5->L+3 (2%), H-3->L+10 (6%), H-2->L+9 (2%), HOMO->L+3 (4%), HOMO->L+5 (4%)
5	39507.72848	253.11	0.0897	H-1->L+1 (30%), HOMO->L+3 (13%),H-11->LUMO (3%), H-4->LUMO (8%), H-4->L+1 (2%), H-3->L+2 (2%), H-2->LUMO (8%), H-2->L+1 (2%), H-1->LUMO (2%), H-1->L+3 (3%), HOMO->L+4 (3%), HOMO->L+5 (4%)
6	40246.53744	248.46	0.0104	H-9->LUMO (55%) H-9->L+3 (5%), H-9->L+5 (4%), H-9->L+11 (3%), H-2->L+6 (2%), H-1->L+5 (3%), H-1->L+6 (7%), H-1->L+7 (5%)
7	41447.50528	241.26	0.0084	HOMO->L+9 (26%), HOMO->L+10 (15%) H-10->L+1 (2%), H-10->L+2 (3%), H-10->L+3 (2%), H-6->L+2 (2%), H-5->L+1 (2%), H-5->L+2 (2%), H-4->L+4 (2%), H-3->L+4 (3%), H-3->L+10 (3%), H-2->L+4 (4%), HOMO->L+7 (2%)
8	41520.09568	240.84	0.0238	HOMO->L+9 (12%), HOMO->L+10 (29%) H-10->L+2 (6%), H-6->L+3 (3%), H-5->L+2 (3%), H-3->L+4 (7%), H-3->L+9 (3%)
9	42250.83904	236.68	0.0024	H-8->L+1 (12%), H-1->L+6 (12%), H-1->L+7 (10%) H-11->L+8 (3%), H-8->LUMO (7%), H-8->L+3 (6%), H-8->L+11 (3%), H-7->L+1 (9%), H-4->L+6 (3%), H-2->L+7 (3%), H-1->L+8 (3%), HOMO->L+6 (2%), HOMO->L+7 (3%), HOMO->L+9 (2%)
10	42629.11568	234.58	0.0001	H-7->L+1 (18%), H-1->L+8 (15%) H-11->L+7 (3%), H-8->LUMO (4%), H-8->L+1 (9%), H-8->L+3 (3%), H-7->L+5 (3%), H-7->L+14 (4%), H-4->L+8 (2%), H-2->L+7 (5%), H-2->L+8 (5%), H-1->L+7 (2%), HOMO->L+7 (2%), HOMO->L+8 (4%), HOMO->L+9 (3%)

Archive of SID

www.SID.ir

Absorption spectrum of 3b at PCM-TD-LC-BLYP/6-31G** level of theory and %age contribution

No.	Energy (cm-1)	Wavelength (nm)	Osc. Strength	Major contribs Minor contribs
1	29474.92864	339.27	2.4146	H-2->LUMO (24%), H-1->LUMO (56%), H-4->LUMO (5%), H-3->LUMO (2%)
2	34688.53248	288.27	1.0675	HOMO->L+1 (42%), HOMO->L+3 (25%) H-3->L+2 (2%), H-2->LUMO (3%), H-2->L+1 (4%), H-1->L+1 (5%)
3	35945.95952	278.19	0.9504	HOMO->L+2 (77%) H-3->L+3 (3%), H-3->L+6 (2%), H-1->L+2 (4%), HOMO->L+15 (3%)
4	38467.26608	259.96	0.0256	HOMO->L+4 (68%) H-6->L+1 (2%), H-6->L+3 (3%), H-5->L+2 (4%), H-3->L+10 (5%), H-2->L+9 (2%)
5	39548.05648	252.85	0.0989	H-1->L+1 (32%), HOMO->L+3 (14%) H-11->LUMO (4%), H-4->LUMO (9%), H-4->L+1 (3%), H-2->LUMO (7%), H-1->LUMO (3%), H-1->L+3 (3%), HOMO->L+6 (2%)
6	40236.05216	248.53	0.0105	H-10->LUMO (55%) H-10->L+3 (6%), H-10->L+6 (3%), H-10->L+11 (3%), H-2->L+5 (3%), H-1->L+5 (8%), H-1->L+7 (5%)
7	41449.1184	241.25	0.0254	HOMO->L+9 (39%) H-9->L+1 (4%), H-9->L+3 (4%), H-6->L+1 (3%), H-6->L+11 (2%), H-5->L+2 (4%), H-4->L+4 (3%), H-4->L+9 (2%), H-3->L+10 (4%), H-2->L+4 (7%), H-1->L+4 (3%), HOMO->L+7 (3%), HOMO->L+8 (3%)
8	41553.9712	240.65	0.0213	H-3->L+4 (11%), HOMO->L+10 (44%) H-13->L+4 (2%), H-9->L+2 (7%), H-6->L+2 (6%), H-5->L+3 (4%), H-5->L+6 (2%), H-3->L+9 (4%), H-2->L+10 (2%), H-1->L+10 (3%)
9	42224.22256	236.83	0.0031	H-8->L+1 (12%), H-7->L+1 (10%) H-14->L+8 (2%), H-11->L+8 (3%), H-8->LUMO (7%), H-8->L+3 (5%), H-8->L+11 (3%), H-4->L+6 (2%), H-2->L+7 (2%), H-1->L+5 (7%), H-1->L+6 (9%), H-1->L+7 (9%), H-1->L+8 (3%), HOMO->L+7 (2%), HOMO->L+9 (2%)
10	42613.79104	234.66	0.0	H-8->L+1 (10%), H-7->L+1 (18%), H-1->L+8 (15%) H-11->L+7 (2%), H-8->LUMO (4%), H-8->L+3 (3%), H-7->L+6 (3%), H-7->L+14 (4%), H-4->L+8 (3%), H-2->L+7 (4%), H-2->L+8 (4%), H-1->L+7 (2%), HOMO->L+7 (2%), HOMO->L+8 (4%), HOMO->L+9 (3%)

Archive of SID

www.SID.ir

Absorption spectrum of 3c at PCM-TD-LC-BLYP/6-31G** level of theory and %age contribution

No.	Energy (cm-1)	Wavelength (nm)	Osc. Strength	Major contribs Minor contribs
1	29478.96144	339.22	2.3956	H-2->LUMO (24%), H-1->LUMO (58%) H-4->LUMO (4%), HOMO->LUMO (2%)
2	35056.32384	285.25	1.0687	HOMO->L+1 (42%), HOMO->L+2 (23%) H-2->LUMO (4%), H-2->L+1 (4%), H-1 >L+1 (5%)
3	37744.58832	264.93	0.7366	HOMO->L+3 (76%) H-2->L+3 (2%), H-1->L+3 (4%), HOMO->L+15 (2%)
4	38775.372	257.89	0.0453	HOMO->L+4 (69%) H-12->L+10 (2%), H-6->L+1 (2%), H-6->L+2 (2%), H-5->L+3 (3%), H-3->L+10 (3%), H-2->L+9 (3%)
5	39802.92944	251.23	0.0837	H-1->L+1 (31%), HOMO->L+2 (13%) H-9->LUMO (6%), H-4->LUMO (8%), H-4->L+1 (3%), H-2->LUMO (8%), H-1->LUMO (3%), H-1->L+2 (3%), HOMO->L+7 (3%)
6	40236.85872	248.52	0.0108	H-11->LUMO (55%), H-1->L+5 (11%) H-11->L+2 (7%), H-11->L+7 (3%), H-2->L+5 (3%), H-1->L+6 (3%), H-1->L+8 (2%)
7	41673.34208	239.96	0.0354	HOMO->L+9 (38%) H-10->L+1 (3%), H-10->L+2(4%), H-9->L+4 (3%), H-6->L+11 (2%), H-5->L+3 (5%), H-3->L+10 (4%), H-2->L+4 (6%), H-1->L+4 (3%), HOMO->L+6 (4%), HOMO->L+8 (2%)
8	42141.95344	237.29	0.0234	HOMO->L+10 (45%) H-12->L+4 (4%), H-10->L+3 (7%), H-6->L+3 (6%), H-5->L+2 (2%), H-5->L+7 (2%), H-3->L+4 (9%), H-3->L+9 (3%), H-2->L+10 (3%), H-1->L+10 (4%)
9	42231.4816	236.79	0.0048	H-8->L+1 (13%), H-1->L+5 (11%), H-1->L+6 (12%) H-8->LUMO (7%), H-8->L+2 (5%), H-8->L+11 (3%), H-7->L+1 (9%), H-4->L+5 (2%), H-4->L+6 (2%), H-2->L+6 (3%), H-1->L+8 (3%), HOMO->L+6 (3%), HOMO->L+9 (3%)
10	42616.21072	234.65	0.0001	H-8->L+1 (10%), H-7->L+1 (18%), H-8->LUMO (4%), H-8->L+2 (2%), H-7->L+14 (3%), H-2->L+6 (4%), H-2->L+7 (3%), H-1->L+7 (8%), H-1->L+8 (8%), HOMO->L+6 (2%), HOMO->L+7 (3%), HOMO->L+9 (4%)

Absorption spectrum of 3d at PCM-TD-LC-BLYP/6-31G** level of theory and %age contribution

No.	Energy (cm-1)	Wavelength (nm)	Osc. Strength	Major contribs Minor contribs
1	29466.05648	339.37	2.3996	H-2->LUMO (18%), H-1->LUMO (57%) H-4->LUMO (6%), H-3->LUMO (4%), HOMO->LUMO (2%)
2	35075.68128	285.09	1.0743	HOMO->L+1 (42%), HOMO->L+2 (23%) H-2->LUMO (3%), H-2->L+1 (3%), H-1->L+1 (6%), HOMO->L+8 (3%)
3	38397.09536	260.43	0.6058	HOMO->L+3 (75%) H-1->L+3 (4%)
4	38847.15584	257.41	0.1675	HOMO->L+4 (68%) H-11->L+10 (2%), H-6->L+2 (2%), H-5->L+3 (2%), HOMO->L+3 (2%)
5	39841.64432	250.99	0.0755	H-1->L+1 (31%), HOMO->L+2 (13%) H-13->LUMO (2%), H-8->LUMO (7%), H-4->LUMO (6%), H-4->L+1 (3%), H-2->LUMO (5%), H-1->LUMO (3%), H-1->L+2 (3%), HOMO->L+8 (6%)
6	40232.01936	248.55	0.011	H-12->LUMO (55%), H-1->L+5 (11%) H-12->L+2 (8%), H-12->L+8 (4%), H-2->L+5 (2%), H-1->L+6 (4%)
7	41707.2176	239.76	0.0414	HOMO->L+9 (38%) H-11->L+10 (3%), H-10->L+1 (3%), H-10->L+2 (3%), H-8->L+4 (4%), H-7->L+1 (2%), H-5->L+3 (6%), H-3->L+10 (2%), H-2->L+4 (5%), H-1->L+4 (2%), HOMO->L+6 (4%), HOMO->L+7 (4%)
8	42216.96352	236.87	0.0053	H-9->L+1 (13%), H-1->L+5 (11%), H-1->L+6 (12%) H-9->LUMO (7%), H-9->L+2 (5%), H-9->L+11 (3%), H-8->L+7 (3%), H-7->L+1 (9%), H-4->L+6 (2%), H-1->L+7 (2%), HOMO->L+5 (2%), HOMO->L+6 (3%), HOMO->L+9 (4%)
9	42303.26544	236.38	0.0249	HOMO->L+10 (45%) H-11->L+4 (4%), H-11->L+9 (2%), H-10->L+3 (7%), H-6->L+3 (4%), H-6->L+4 (2%), H-5->L+8 (3%), H-3->L+4 (6%), H-3->L+9 (2%), H-1->L+10 (4%)
10	42608.14512	234.69	0.0001	H-9->L+1 (10%), H-7->L+1 (17%), H-1->L+7 (15%) H-13->L+6 (2%), H-9->LUMO (4%), H-7->L+8 (3%), H-7->L+14 (3%), H-4->L+7 (3%), H-2->L+6 (3%), H-2->L+7 (3%), HOMO->L+6 (2%), HOMO->L+7 (5%), HOMO->L+9 (4%)

Archive of SID

www.SID.ir